Pedestrian Kernel Density Estimates: the Individual Approach

Jana Vacková and Marek Bukáček

Abstract The pedestrian density evaluation problem can be generally perceived as a sampling exercise. Assuming a density distribution inside the analysed area is already generated, the task is to generate a number characterizing the state of an area (detector estimates) or the surroundings of a pedestrian (individual approach). Application of individual density may be crucial e.g. to calibrate any microscopic model or to measure any interaction between pedestrians. Thus, this contribution deals with the individual concept using a conic kernel to generate the density distribution ensuring a pedestrian blurring with great performance. Then the density in pedestrian surroundings of an arbitrary shape with a specific range for a specific pedestrian is defined using kernel distributions. The influence of the shape of pedestrian surroundings and its size described by parameter r are presented using quantitative metrics. The following type of surroundings (using a different r) are examined: circle (radius); ellipse (length of semi-axes) and sector (radius, angle) which are rotated in accordance with a direction of a pedestrian movement.

Keywords: Pedestrian dynamics, Density, Pedestrian surroundings, Individual density, Kernel function, Density distribution

1 Introduction

Flow, velocity and density are considered to be fundamental quantities in both traffic flow, e.g. [9], and pedestrian dynamics, e.g. [4, 7]. The standard approach using physical definitions of flow and density as counting the number of pedestrians $\mathcal{N}$ passing through a cross-section within the interval ΔT or standing in the area $\mathcal{A}$ enriched by the hydrodynamic approximation $J = \rho \cdot v$ was widely studied

Jana Vackova´
FNSPE Czech Technical University in Prague, Trojanova 13, Prague, Czechia, e-mail: janca.vackova@fjfi.cvut.cz

Marek Bukáček
FNSPE Czech Technical University in Prague, Trojanova 13, Prague, Czechia e-mail: marek.bukacek@seznam.cz

K. R. Rao et al. (eds.), *Traffic and Granular Flow '22* , Lecture Notes in Civil Engineering 443, https://doi.org/10.1007/978-981-99-7976-9_17

throughout the decades. However, the estimates of these fundamental quantities are still developing [5].

Kernel estimates for the calculation of pedestrian density that we have applied in [2, 10, 3] were first introduced in [8]. Those kernels were used to generate density distribution in the room that enables the evaluation of density in any particular area, as we presented in [11] where a static detector was examined. In this paper, we will extend conducted research focusing on the impact of the shape and the size of pedestrian surroundings on density output. Compared to [11], the dynamic detector is used here which is dynamically changing its position in accordance with the pedestrian position at every time step.

Individual density is needed due to the possibility to capture local information from the pedestrian perspective. This approach can bring new and important insights into the measuring of behaviour in an observed area. First, a comparison of the static and dynamic detectors will be provided, demonstrating the importance to be local. Then the effects of different surrounding shapes (circle, sector, ellipse) will be examined. Finally, the elliptic density correspondence to sectors' density will be provided.

The following parametric study is based on the egress experiment organized in the study hall of FNSPE, CTU in Prague in 2014, for details see [1]. Pedestrians (undergraduate students) entered the room by one of three entrances, walked to the opposite wall and left the room by one exit. They were instructed to leave the room as fast as possible without running or any strong physical contact. In total, our sample is made up of 2000 paths through 10 experimental rounds captured using 48 frames per second.

2 Individual Concept Definition

Every single pedestrian is assumed to be a source of *individual density distribution*. Rewrite the definition of *density* in an area $A \subset \mathbf{R}^2$

$$\rho_A = \frac{N}{|A|} = \frac{\int_A p(\boldsymbol{x})\,\mathrm{d}\boldsymbol{x}}{|A|} = \frac{\int_A \sum_{\alpha=1}^{N} p_\alpha(\boldsymbol{x})\,\mathrm{d}\boldsymbol{x}}{|A|} = \sum_{\alpha=1}^{N} \frac{\int_A p_\alpha(\boldsymbol{x})\,\mathrm{d}\boldsymbol{x}}{|A|}, \tag{1}$$

where $N \in \mathbf{N}_0$ represents the total (discrete) number of pedestrians, $|A|$ the size of considered area A, $p_\alpha(\boldsymbol{x})$ the *individual density distribution* generated by each pedestrian $\alpha \in \{1, 2, \ldots, N\}$ and $p(\boldsymbol{x}) = \sum_{\alpha=1}^{N} p_\alpha(\boldsymbol{x})$ the *density distribution* in the area A. The usage of kernel functions for pedestrian density estimates are deeply discussed in [11].

We denote *static detector (global) density* as ρ_A. On the contrary, the *individual density* ρ_α for a specific pedestrian α with dynamic pedestrian surroundings ω_α is defined as follows

$$\rho_\alpha = \frac{\int_{\omega_\alpha(\boldsymbol{r})} \sum_{\beta=1,\beta\neq\alpha}^{N} p_\beta(\boldsymbol{x}, R)\,\mathrm{d}\boldsymbol{x}}{|\omega_\alpha(\boldsymbol{r})|}. \tag{2}$$

Regardless of the kernel type, $R \in \mathbf{R}$ expresses the smoothing factor and $\boldsymbol{r} \in \mathbf{R}^n$, where $n \in \mathbf{N}$, represents the pedestrian range. Thus we refer to it as a *blur* and a *range* respectively. Blur[1] $R \in \mathbf{R}$ controls the size of an area affected by one pedestrian. Range $\boldsymbol{r} \in \mathbf{R}^n$, where $n \in \mathbf{N}$, controls the size of pedestrian surroundings defining the area taken into account for evaluating the density. Its dimension can vary, we will use $n = 1$ or $n = 2$ for specific surroundings shapes defined in the following text.

Clearly we exclude the individual density distribution of the pedestrian α in the individual approach (2), i.e. the pedestrian α does not contribute to the density in their surroundings. The reason is if there is not any other pedestrian near the pedestrian α, the individual density is equal to zero. If we did not exclude the pedestrian α, the individual density would be equal to the mass of the pedestrian α. For instance, the pedestrian mass is represented by conic kernel with blur R and the individual density is computed in the circular surroundings $\omega_\alpha(r)$ with radius $r \in \mathbf{R}$, then $\rho_{\omega_\alpha(r)} = \frac{1}{\pi r^2}$ ped/m^2 for $R \leq r$ and any other pedestrian represented at least $r + R$ m far away.

In this paper, we assume density distribution $p(\boldsymbol{x}, R)$ using conic kernel with the radius of the base $R = 0.9$ m (according to the results obtained in [11]), see Fig. 1. Different types (shapes and sizes) of the pedestrian surroundings can be used; the types used in this study are defined in the following subsection. The static detector A for computing ρ_A of size 2 m^2 is located (and centred) at the exit area.

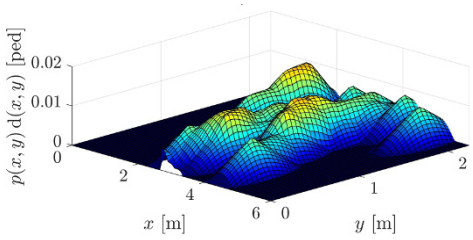

Fig. 1 An example of density distribution $p(\boldsymbol{x})$ in an observed area using conic kernel with $R = 0.9$ m.

2.1 Types of Pedestrian Surroundings

Having introduced the individual density of pedestrian α (2), we need to specify the shape of the pedestrian surroundings in the meaning of the dynamic detector. The choice of the specific shape is very promising in the bending of the definition (2) for a specific purpose from the microscopic point of view.

[1] Note that blur can be more-dimensional parameter for non-symmetric kernels. However, we will use solely symmetric kernels in this paper.

We remark our notation at fixed time t for the (head) position $\boldsymbol{x}_\alpha = (x_{\alpha,1}, x_{\alpha,2}) := \boldsymbol{x}_\alpha(t)$ of pedestrian α, current velocity $\boldsymbol{v}_\alpha := \boldsymbol{v}_\alpha(t)$ of pedestrian α and the surroundings $\omega_\alpha(\boldsymbol{r}) := \omega_\alpha(\boldsymbol{r}, t)$ of pedestrian α, where $\boldsymbol{r}$ can be an arbitrary range parameter ($\boldsymbol{r}$ can be one-dimensional or two-dimensional) defining the specific surrounding as follows.

Circle with range defined as radius $r > 0$ of the circle can be written as

$$\omega_\alpha(r) = \left\{\boldsymbol{x} \in \mathbf{R}^2 : \|\boldsymbol{x} - \boldsymbol{x}_\alpha\| \leq r\right\}.$$

Circular sector with range $\boldsymbol{r} = (r, \gamma)$, where $\gamma \in (0, \pi\rangle$ is central angle and $r > 0$ is radius, is defined as follows

$$\omega_\alpha(r, \gamma) = \left\{\boldsymbol{x} \in \mathbf{R}^2 : \|\boldsymbol{x} - \boldsymbol{x}_\alpha\| \leq r \wedge \measuredangle(\boldsymbol{x} - \boldsymbol{x}_\alpha, \boldsymbol{v}_\alpha) \leq \frac{\gamma}{2}\right\}.$$

The sector is rotated in the pedestrian movement direction.

Ellipse with $\boldsymbol{r} = (a, b)$, $a > b$, where $a \in \mathbf{R}^+$ is the length of semi-mayor axis and $b \in \mathbf{R}^+$ the length of semi-minor axis. The ellipse is rotated into the current pedestrian movement direction and the pedestrian is located into the first focus of the ellipse; the second focus lies right ahead of them.

The shapes of all defined surroundings are depicted in Fig. 2.

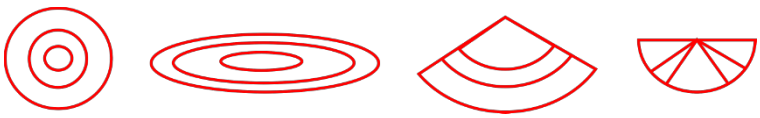

Fig. 2 Type of pedestrian surroundings used in this study.

3 Importance of Being Local

For the first impression, the most basic (circular) surroundings are applied to compare the detector and individual approach; four chosen time frames are depicted in Fig. 3. Coloured points are located at the pedestrian's head positions, dotted circles represent specific ($r = 0.5$ m) circular surroundings and static detector density $\rho_A(t)$ is visualised at the top left coloured square. There are visible differences between detector density and individual density, e.g. see the fourth time frame with very high static detector density and quite low individual densities in the detector. Although high congestion is detected, pedestrians individually differ from this value in the detector area.

Note that ρ_A is constantly higher approx. 0.5 ped/m^2 than ρ_α because the chosen pedestrian α is excluded in the definition of their individual density (2), thus the individual density is constantly $1/|A|$ lower than the static density in this detector A.

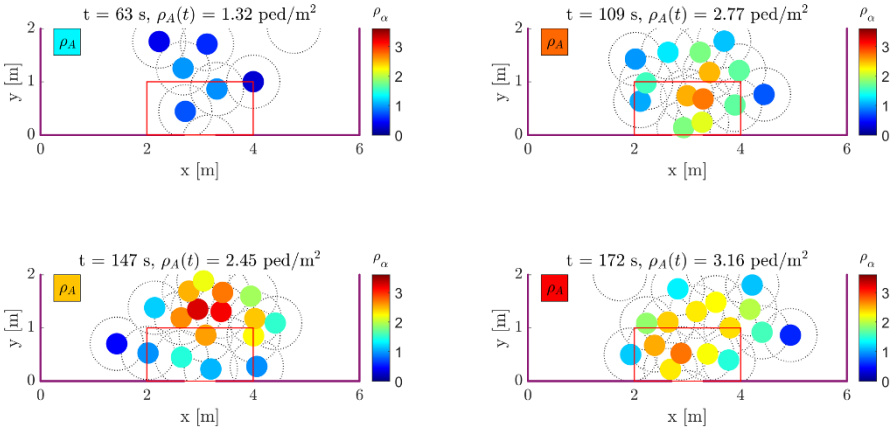

Fig. 3 Static detector density $\rho_A(t)$ (top left coloured square) versus pedestrian individual density $\rho_\alpha(t)$ (using circular surroundings with range $r = 0.5$ m).

4 Impact of Range and Surroundings Shape on the Indiv. Density

To cover more than a few time frames, trajectories from the experimental round 6 are plotted in Fig. 4. Only trajectories from the steady state are used to be sure the results are not affected by random drops. The trend of static detector density is shown at the top. Strongly blurred results can be seen using $r = 1$ m; on the contrary, little blurred results are obtained using $r = 0.2$ m or $r = 0.5$ m. Therefore the individual density with range $r = 1$ m cannot detect expected density peaks and density downs due to high blurring and the additive information sublimed. However, the individual density with a lower range can detect density fluctuations and bring desired individual (and local) information. Note that range r greater than 1 m is not suitable to be compared with our detector of size 2 m^2.

Fig. 5 compares locally the time development of global density ρ_A (black) and chosen individual densities ρ_α (colors) measured for specific pedestrian $\alpha = 1240$; various types of surroundings and parameters are visualized. The global density in the detector A (during the passage of pedestrian α) is almost constant. On the contrary, a more pronounced trend is observed even using a circular shape. Moreover, the lower the central angle of the sector is, the more noticeable the density peak is. And at the same time, the lower the radius of the sector is, the minor the change is in density when using different central angles of the sector.

Analogously, the time development for an ellipse can be seen in Fig. 6. It is possible to obtain similar results to the circle and sectors using specific values of the elliptic axes. This behaviour was expected due to the elliptic definition and we will examine it in general (for any pedestrian and any trajectory) in the further section.

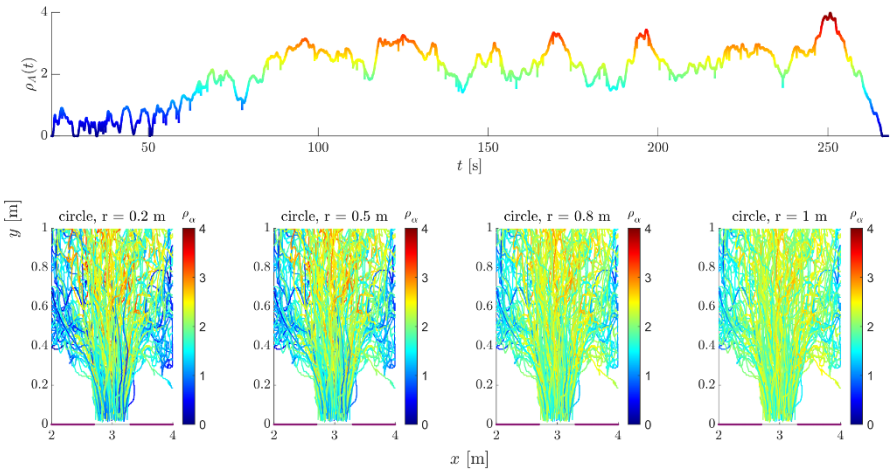

Fig. 4 Detector density $\rho_A(t)$ versus coloured pedestrian trajectories using $\rho_\alpha(t)$ of the experimental round (number 6, stable cluster) for different values of circular range r.

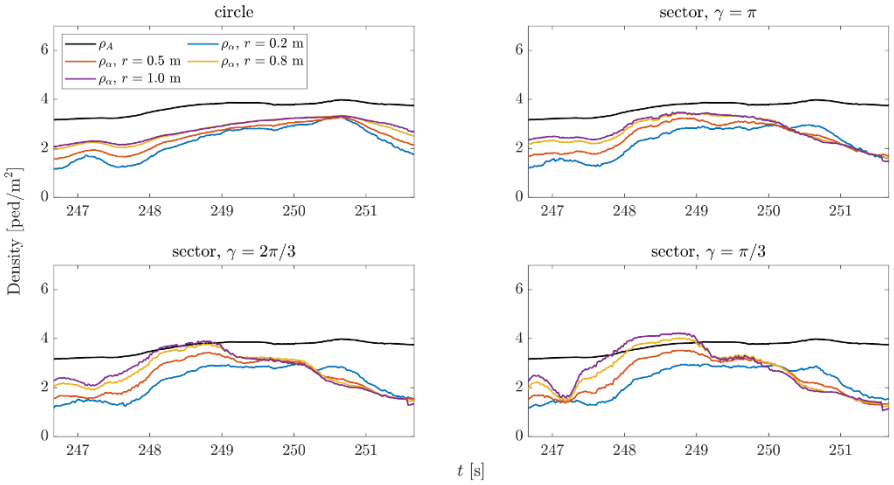

Fig. 5 Time development of ρ_A and ρ_α for specific pedestrian α = 1240 (circle, sectors).

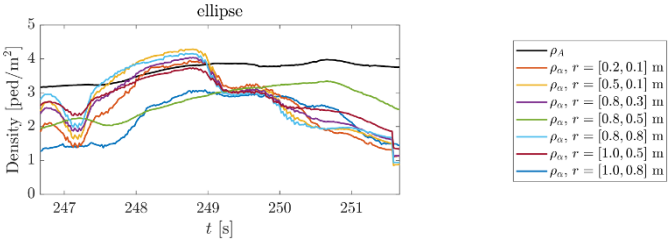

Fig. 6 Time development of ρ_A and ρ_α for specific pedestrian α = 1240 (ellipse).

5 Elliptic Correspondence to Sectors

Having the preliminary results, we expect a correspondence between elliptic density and other shapes of surroundings, i.e. elliptic parametric settings ensuring the similarity of densities exists. It is clear that an ellipse with $a = b$ is transformed into a circle with radius $r = a = b$. For these reasons, only the correspondence between ellipse and sectors will be checked quantitatively.

The density distribution from (1) ensures the propagation of pedestrian influence into any shape of surroundings. Thus finding any correspondence between a sector and an ellipse is reasonable despite the fact that the ellipse 'sees behind the pedestrian' and the sector does not.

A corresponding ellipse is found for each sector using the minimization of mean absolute deviation between their density curves using data of the experimental round number 6 (more than 250 trajectories). The correspondence is studied using the ratio of the length of elliptic axes a/b, the central angle of sector γ and the areas of surroundings, see Fig. 7. The area of the fixed sector and the area of the corresponding ellipse does not differ significantly (variances for the mean semi-mayor axis and the mean semi-minor axis are less than 10^{-2} m^2). Besides, a narrow ellipse corresponds to sectors with low central angles and an ellipse with $a \approx b$ is the closest option for a semicircle.

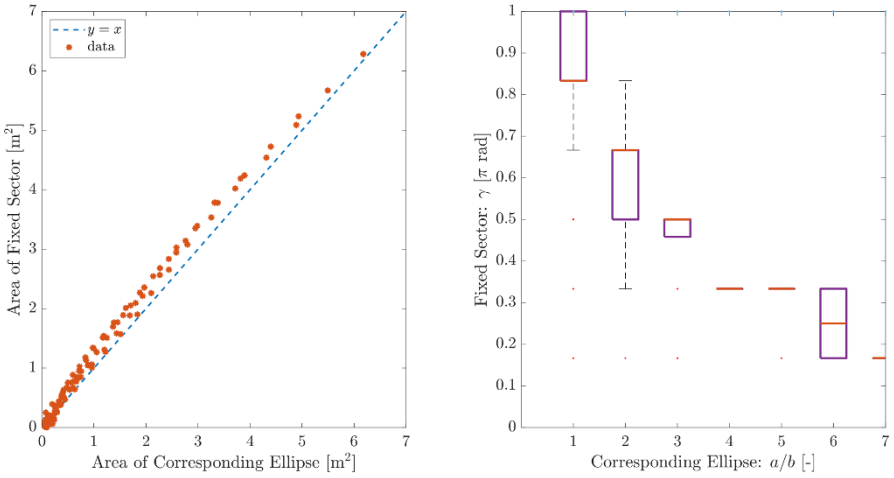

Fig. 7 Comparison of area and axis ratio for corresponding ellipse and sector. Data of all pedestrians from experimental round number 6 was used.

6 Conclusions

The introduced individual approach gives a new possibility of insight into pedestrian dynamics, besides the global (static detector) density. As was shown in this contribution, the individual density brings additive information about dynamics in an observed area (including specific pedestrian conditions in their surroundings) that cannot be observable using the static detector density.

Circular surroundings useful for modelling the proxemics zone established by Hall [6] can be considered as the simplest case, however, we went much deeper. More individual information is brought by elliptic surroundings covering an area mostly in front of the pedestrian and to some extent also behind the pedestrian, and shape defined by sector with specific central angle representing the visual field of the pedestrian. All possible properties of examining types are gathered in the elliptic shape due to its generality. Although the size of the specific surroundings differs concerning the current application, it can be chosen according to the desired characteristics.

To conclude, individual density brings new information about conditions in the observed area using any type of pedestrian surroundings. Elliptic surroundings have the most general properties, thus we recommend using them.

References

1. Marek Bukáček, Pavel Hrabák, and Milan Krbálek. Microscopic travel-time analysis of bottleneck experiments. *Transportmetrica A: transport science*, 14(5-6):375–391, 2018.
2. Marek Bukáček and Jana Vacková. Evaluation of pedestrian density distribution with respect to the velocity response. In *Traffic and Granular Flow'17*. Springer, 2019.
3. Marek Bukáček and Jana Vacková. Density estimates in cellular automata models of pedestrian dynamics. In Bastien Chopard, Stefania Bandini, Alberto Dennunzio, and Mira Arabi Haddad, editors, *Cellular Automata*, pages 271–280, Cham, 2022. Springer International Publishing.
4. Winnie Daamen and Serge P Hoogendoorn. Flow-density relations for pedestrian traffic. In *Traffic and granular flow'05*, pages 315–322. Springer, 2007.
5. Dorine C Duives, Winnie Daamen, and Serge P Hoogendoorn. Quantification of the level of crowdedness for pedestrian movements. *Physica A: Statistical Mechanics and its Applications*, 427:162–180, 2015.
6. E.T. Hall. The silent language. 1959.
7. Andreas Schadschneider, Mohcine Chraibi, Armin Seyfried, Antoine Tordeux, and Jun Zhang. Pedestrian dynamics: From empirical results to modeling. In *Crowd Dynamics, Volume 1*, pages 63–102. Springer, 2018.
8. Bernhard Steffen and Armin Seyfried. Methods for measuring pedestrian density, flow, speed and direction with minimal scatter. *Physica A: Statistical mechanics and its applications*, 389(9):1902–1910, 2010.
9. Martin Treiber and Arne Kesting. Traffic flow dynamics. *Traffic Flow Dynamics: Data, Models and Simulation, Springer-Verlag Berlin Heidelberg*, 2013.
10. Jana Vacková and Marek Bukáček. Follower-leader concept in microscopic analysis of pedestrian movement in a crowd. In *Pedestrian and Evacuation Dynamics 2018*. Collective Dynamics, 2020.
11. Jana Vacková and Marek Bukáček. Kernel estimates as general concept for the measuring of pedestrian density. *arXiv preprint arXiv:2205.10145*, 2022.